ELSEVIER

Gait and Posture 12 (2000) 225–234

GAIT & POSTURE

www.elsevier.com/locate/gaitpost

An improved technique for the extraction of stochastic parameters from stabilograms

Lorenzo Chiari [a,*], Angelo Cappello [a], Davide Lenzi [a], Ugo Della Croce [b]

[a] *Biomedical Engineering Unit, Department of Electronics, Computer Science and Systems, University of Bologna, Viale Risorgimento 2, I-40136 Bologna, Italy*

[b] *Biomedical Sciences Department, University of Sassari, Sassari, Italy*

Accepted 20 August 2000

Abstract

An improved characterization of the dynamics of postural sway can provide a better understanding about the functional organization of the postural control system as well as a more robust tool for postural pattern recognition. To this aim, a novel parameterization was applied to the stabilogram diffusion analysis formerly proposed by Collins and De Luca [Collins JJ, De Luca CJ. Open-loop and closed-loop control of posture: a random-walk analysis of center-of-pressure trajectories. Exp Brain Res 1993;95:308–18] that considered the act of maintaining posture as a stochastic process. The main purpose of the present technique was to overcome some drawbacks of the model presented by Collins and De Luca that may restrain its potential application in clinical practice. The approach uses a unique non-linear model to describe the center of pressure (COP) dynamics that reduces the number of parameters and decreases their intra-subject variability; consequently, fewer trials are required to perform reliable estimates of stochastic parameters and this is of particular importance for subjects that cannot afford many repeated measurements because of age or pathology. Four new statistical mechanics parameters (NSMP) were computed on the log–log stabilogram diffusion plots and their estimates were compared in terms of reliability and sensitivity to the visual conditions with: (1) a minimal set of four summary statistic scores (SSS); and (2) the six statistical mechanics parameters (SMP) proposed by Collins and De Luca. All four NSMP showed at least a fair-to-good reliability (intraclass correlation coefficient, ICC > 0.49) while SMP (ICC > 0.20) showed some poor reliability. A better overall reliability was also observed with respect to SSS. Moreover, only NSMP had a similar score for eyes open and eyes closed conditions. Three out of four NSMP were also significantly sensitive to eyes open or closed conditions ($P < 0.001$) while only three out of six SMP were sensitive to operating conditions ($P < 0.01$).

Keywords: Control of posture; Parameter estimation; Platform stabilometry; Stochastic model; Vision

1. Introduction

Upright posture is commonly investigated to provide information about motor ability in patients [1–4] and in the elderly [5–8], both in static and dynamic conditions. Nevertheless, the clinical effectiveness of relevant tests is often limited by the difficulty of extracting meaningful and reliable parameters.

Posture is often analyzed by means of a force platform, which provides the apparently erratic time-course of the center of pressure (COP), commonly referred to as 'statokinesigram' [9] (Fig. 1 — Top). Several methods have been proposed in the past for the calculation of posturographic parameters from COP trajectories. Many former studies were limited to the analysis of these plots using summary statistic scores, such as time-domain distance, area and hybrid measures, and frequency domain measures [7]. These parameters tend to have reasonable reliability but limited sensitivity [3,10] and do not consider the dynamic properties of the stabilogram.

In contrast, some researchers attempted to characterize COP motion over the base of support through different models of its governing dynamics, assuming posture as the dynamic stability of a continuously swaying body. A deterministic approach led Yamada

* Corresponding author. Tel.: +39-051-2093014; fax: +39-051-2093073.

E-mail address: lchiari@deis.unibo.it (L. Chiari).

0966-6362/00/$ - see front matter
PII: S0966-6362(00)00086-2

[11] to describe the fluctuation of the COP as a chaotic process, while Collins and De Luca [12] considered the signal to be one of the realizations of a particular stochastic process. Up to now, the stochastic hypothesis has been popular in literature for the relevant role assumed by physiological noise in static posturography, since neural control signals are always corrupted by noise, the variance of which is proportional to the size of the signal [13].

Collins and De Luca described the stochastic properties of the COP dynamics through statistical mechanics parameters (SMP) using a two-process, random-walk model. By assuming that the COP trajectory is a correlated random-walk, they brought out a short-term (s) process and a long-term (l) process altogether described by a set of six parameters in the form of the following:

- critical point coordinates, $(\Delta t_c, \langle \Delta r^2 \rangle_c)$, separating the dynamics in a short-term and a long-term region; and, for each region,
- a diffusion coefficient, D, descending from Einstein's law for classical Brownian motion,

$$< \Delta r^2 \geq 2D\ \Delta t \quad (1)$$

- a scaling exponent, H, descending from generalization of Eq. (1) for fractional Brownian motion ($0 \leq H \leq 1$),

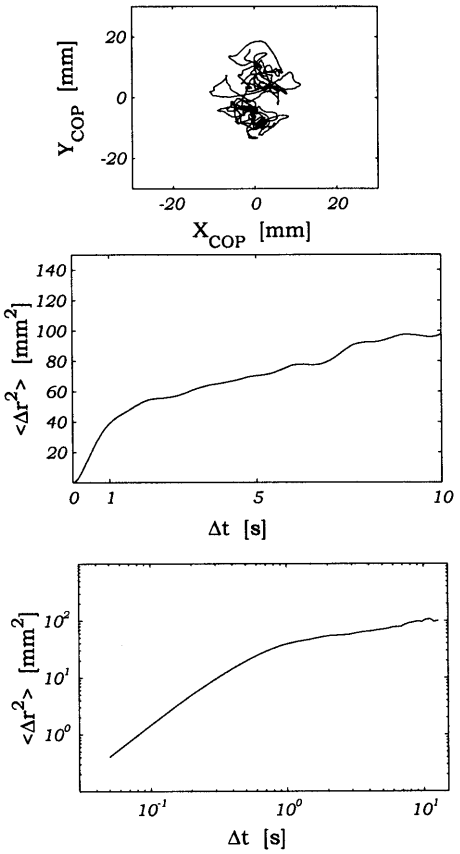

Fig. 1. Top — Representative 50 s statokinesigram recorded with eyes open. Middle — Resultant planar stabilogram diffusion plot generated according to the method proposed by Collins and De Luca [12] represented in linear coordinates. Bottom — The same stabilogram diffusion plot in double logarithmic coordinates.

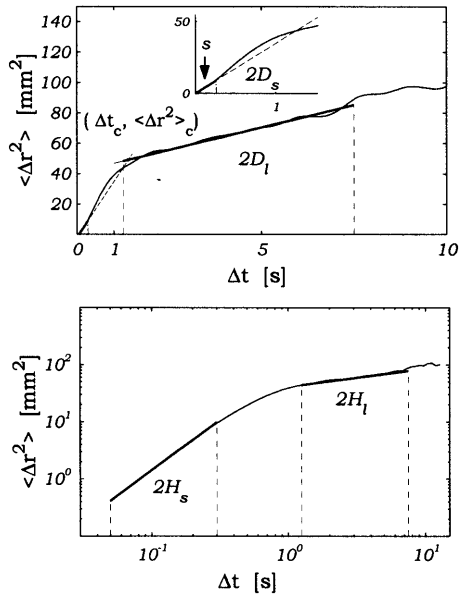

Fig. 2. Top — Graphical representation of the four SMP parameters extracted from the planar stabilogram diffusion plot represented in linear coordinates. D_s and D_l are the diffusion coefficients and $(\Delta t_c, \langle \Delta r^2 \rangle_c)$ are the critical point coordinates. The short-term region is zoomed in the small panel. Bottom — Graphical representation of the two SMP parameters extracted from the planar stabilogram diffusion plot in double logarithmic coordinates. The scaling exponents H_s and H_l are computed from the slopes of the lines fitted to the short-term and long-term regions identified in the linear plane.

$$< \Delta r^2 > \sim \Delta t^{2H} \quad (2)$$

In Eqs. (1) and (2), $\langle \Delta r^2 \rangle$ represents the mean square planar displacement between all pairs of points of the statokinesigram separated by the time interval Δt. The plots of $\langle \Delta r^2 \rangle$ versus Δt, computed from COP time-series, are commonly referred to as 'stabilogram diffusion plots' (SDP) and can be represented both in linear and logarithmic scale to enable the estimation of the aforementioned parameters. Fig. 1 shows a representative statokinesigram and the corresponding linear and logarithmic stabilogram diffusion plots. The s and l regions are in this case well evident both in the linear (Fig. 1 — middle) and logarithmic (Fig. 1 — bottom) plane.

Hence, in short, four parameters are needed for the full characterization of the linear SDP through two straight lines: the two slopes (D_s and D_l) and the two coordinates of their intersection $(\Delta t_c, \langle \Delta r^2 \rangle_c)$. Moreover, two parameters describe the slopes (H_s and H_l) of the straight lines used to fit the logarithmic SDP in the two regions delimited by $(\Delta t_c, \langle \Delta r^2 \rangle_c)$. The graphical representation of these six parameters is proposed in Fig. 2.

Though promising in terms of physiological interpretation of the results and clinical applicability [10,14], this method still shows three main drawbacks. First, the model is not parsimonious, so that the variability in all the parameter estimates can be hopefully reduced (Ref. [15], page 161). Second, the joint use of classical and fractional Brownian motion may create confusion re-

garding the assumptions made and the interpretation of the results. The authors themselves argued that 'the non-linear data-analysis technique' carried out according to Eq. (2) 'is more valid than the linear data-analysis technique' (Ref. [16], page 155). This was the reason why they introduced the concept of 'effective', instead of 'actual', diffusion coefficients. Third, the proposed averaged curve-fitting procedure is time costly because it involves at least ten trials to obtain a parameter estimate.

For this reason, an improved technique has been developed that reduces the number of parameters needed to characterize the data set by assuming a unified theory in which a single model approach is used to fit the log–log stabilogram diffusion plot [17]. In the present paper, this technique is presented and four new statistical mechanics parameters (NSMP) are compared with the six SMP and with a selection of four summary statistic scores (SSS), in terms of intra-individual repeatability and sensitivity to operating conditions during the classic Romberg test [1]. COP parameters with high repeatability eliminate the need of trial averaging, and this is of particular importance for reducing the time needed for testing subjects that cannot afford many repeated measurements because of age or pathology.

2. Materials and methods

2.1. Experimental methods

Experiments were carried out on 12 subjects (six females and six males; age 26–40 years) while assuming a standardized upright posture with arms at the side. Subjects were instructed to look at a circular achromatic target, with a diameter of 3 cm, placed at eye height, about 3 m from the platform, and to stand in a comfortable stance. No other stabilizing tasks were given to the subjects. Trials were performed with eyes open (eo) and eyes closed (ec). None of the subjects had evidence or known history of neuro-musculo-skeletal disorder. Informed consent was obtained prior to the inclusion in the study.

Each subject performed one session with ten trials, each consisting of a 50-s acquisition, after a rest period of approximately 60 s. Each trial in normal visual conditions was followed by a trial with eyes closed. COP coordinates were measured by a multi-component strain gauge force platform (mod.4060-08, Bertec Corporation) and sampled at a frequency of 20 Hz.

2.2. Summary statistic COP parameters

For comparison, a set of four SSS was computed from the bidimensional time series of the COP, chosen on the basis of the findings of Prieto et al. [7]. Mean velocity (MV), 95% confidence ellipse area (CEA), fractal dimension (FD) and centroidal frequency (CF) are uncorrelated measures that may characterize different aspects of postural steadiness. Mean velocity is a very common distance measure and provides an estimate of the average velocity of the COP. The 95% confidence ellipse area is the area of the 95% bivariate confidence ellipse that is expected to enclose approximately 95% of the points on the COP path. The fractal dimension is a generalization of the integer dimension and has fractional, non-integer values. It is a dimensionless measure of the degree to which the statokinesigram fills the bidimensional metric space that it encompasses. The fractal dimension ranges between 1 and 2. It is 1 when the structure is a simple straight or curved line, and fills almost no space. When a structure fills all available space, such as the whole region of stability on the plane of the platform, its fractal dimension is 2. It was computed with the algorithm proposed by Katz and George [18]. Finally, centroidal frequency is the zero crossing frequency of the displacement of the COP, i.e. one-half the mean number of zero crossings per second of the time series [7]. Both MV and CEA have been traditionally used to investigate posture control in many clinical studies, while FD and CF have been proposed and used more recently (e.g. see Prieto et al. [7]). All of them are defined in Table 1.

2.3. A simplified stochastic model

The NSMP were obtained from a single model of bidimensional fractional Brownian motion described by:

$$\langle \Delta r^2 \rangle = 2D\ V_H\ \Delta t^{2H} \tag{3}$$

where V_H is a non-linear function [17] of scaling exponent H, which is equal to 1 when $H = 0.5$. V_H is almost parabolic with upward concavity and is nearly flat around the minimum between $H = 0.5$ and $H = 0.7$. It becomes greater than 1.2 below $H = 0.4$ and above $H = 0.8$. Parameters D and H are time-lag dependent. From such a model it is immediate to obtain Eq. (1), when $H = 0.5$, and the link with Eq. (2) is straightforward. Hence, the physical meaning of parameters D and H remains unchanged in terms of a diffusion coefficient and a scaling exponent, as compared to Collins and De Luca [19].

The displacement analysis of COP trajectories was performed in the range $\Delta t = 0.05$–12.8 s. A logarithmic spacing (56 time lag values) was used to avoid the extreme clustering of points that a linear spacing would produce in the long-term region and the consequent biased estimation of parameters. Since a purely logarithmic spacing between data points was not possible due to the sampling strategy, which is based on a linear

Table 1
SSS considered in the analysis[a]

Parameter	Symbol	Definition
Mean velocity	MV	$\frac{\Sigma_{i=1}^{N-1}\Delta r_i}{T}$
95% Confidence ellipse area	CEA	$6\pi\sqrt{\left(\frac{\Sigma_{i=1}^{N}x_i^2}{N}\frac{\Sigma_{i=1}^{N}y_i^2}{N}\right)^2-\left(\frac{\Sigma_{i=1}^{N}x_i y_i}{N}\right)^2}$
Fractal dimension	FD	$\frac{\log(N)}{\log(N)+\log\left(\frac{\text{RANGE}}{\Sigma_{i=1}^{N-1}\Delta r_i}\right)}$
Centroidal frequency	CF	$\sqrt{\frac{\Sigma_{m=i}^{j}(m\Delta f)^2 G[m]}{\Sigma_{m=i}^{j}G[m]}}$

[a] Abbreviations: Δf, frequency increment; Δr_i, distance between each pair of consecutive points in the COP time series; $G[\cdot]$, power spectral density; i, j, indices associated with the frequencies 0.15 and 5 Hz; N, number of points; RANGE, maximum distance between any two points of the curve; T, acquisition time; x, y, medio-lateral and antero-posterior time-series.

grid, we chose a partially corrected logarithmic spacing where only the points corresponding to integer multiples of the sampling period were considered. In this way we could work with a number of data points for short time scales, which is almost comparable with that of long time scales and is not unbalanced as if a linear spacing were chosen.

The bidimensional stabilogram diffusion plot shown in Fig. 1 depicts a representative trial in vision conditions. Two best-fitting regions were identified in the log–log plane with a transition region that was not taken into account for parameter estimation due to the considerable variability in the slope (this is not always true: in some trials no transition region is identified). The experimental relationship between mean square displacement, $\langle \Delta r^2 \rangle$, and time lag, Δt, in the log–log plot allows for the estimation of both $K = \log(2D\ V_H)$ and H through linear regression in two quasi-linear regions of the curve (s and l) identified by

$$\log\langle \Delta r^2 \rangle = \begin{cases} 2H_s \log \Delta t + K_s \text{ for } \Delta t \le \Delta t_c \\ 2H_l \log \Delta t + K_l \text{ for } \Delta t > \Delta t_c \end{cases} \quad (4)$$

where the parameters are only four in place of six. Hence, parameter identification of model (Eq. (3)) is carried out by observing that D (and consequently K) and H can be conveniently estimated by isolating the short- and long-term regions of the stabilogram diffusion plot. However it should be noted that the model is single: the identification strategy is piecewise in order to deal with its non-linearity. The geometrical meaning of the new parameters is sketched in Fig. 3. In fact, $2H_s$, $2H_l$ are the slopes of the two best-fitting lines, and K_s, K_l are the intercepts for $\Delta t = 1$ (Eq. (4)).

The critical point coordinates, $(\Delta t_c, \langle \Delta r^2 \rangle_c)$, can be uniquely derived by the non-linear expressions:

$$\Delta t_c = 10^{\frac{K_l - K_s}{2(H_s - H_l)}} \quad (5)$$

$$\langle \Delta r^2 \rangle_c = 10^{K_s} \Delta t_c^{2H_s} = 10^{K_l} \Delta t_c^{2H_l} \quad (6)$$

but, being not independent parameters, they were not further on considered in the simplified stochastic model.

The present definition of K can be compared with the expression for fractional Brownian motion variance proposed by Kaplan and Kuo [20].

2.4. Parameter estimation

The parameter estimation process involves for both stochastic models the preliminary definition of the observation intervals in the two short- and long-term regions. As a consequence, the estimation of slopes and offsets of two best-fitting lines takes place in the short-

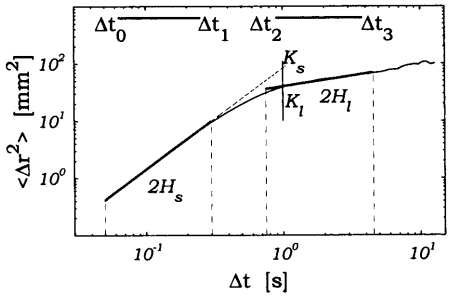

Fig. 3. Graphical representation of the four NSMP parameters. The scaling exponents H_s and H_l are computed from the slopes of the lines fitted to the short-term and long-term regions. The coefficients K_s and K_l are defined by the intersection of such lines with line $\Delta t = 1$. Extremes Δt_i ($i = 0, \ldots, 3$) indicate the time intervals selected for best-fitting.

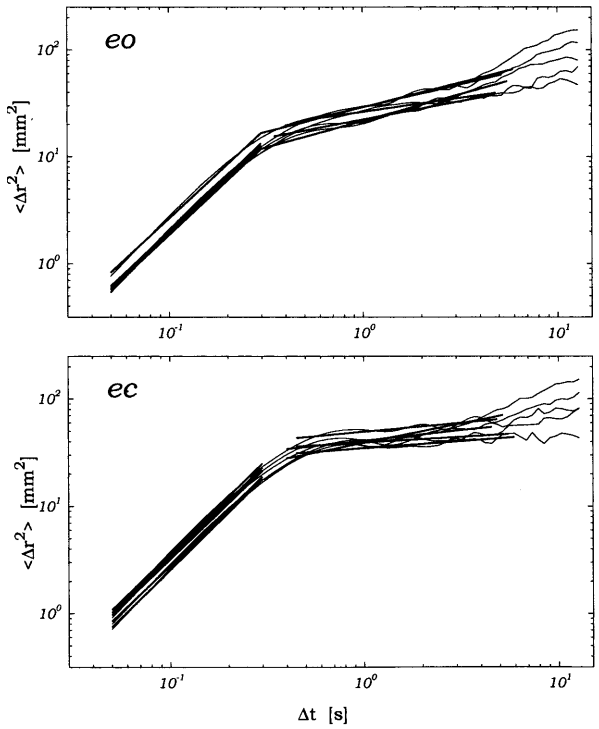

Fig. 4. Stabilogram diffusion plots generated from five different trials of the same subject with eyes open (Top) and eyes closed (Bottom). For each curve the best-fitting lines are shown in bold.

and long-term regions to obtain six SMP through the procedure proposed by Collins and De Luca, or four NSMP from model (Eq. (4)).

2.4.1. Time-interval selection

The shape of the stabilograms is not always regular as the one shown in Fig. 1 (middle and bottom panels). The stochastic nature of the underlying process and the presence of non-stationarity mainly due to low frequency trends in data [21,22] often produce multiple slopes (or even oscillations) in the l region that might mask the main one. This phenomenon is well evident in Fig. 4, where 'all' the stabilograms computed on a subject in eo and ec conditions are shown. The algorithm employed for interval selection consisted of two independent steps concerning the short- and long-term regions of the curves, respectively. In particular, in order to define the l region, a robust algorithm for parameter extraction should look for the quasi-linear tract just after the transition region since longer time lags, characterized by few measurements, are affected by high variance (Fig. 4). In this way, spurious components due to finite size effects can be ignored thus improving the repeatability without using ensemble averages.

2.4.1.1. Short-term working region. The s region ($\Delta t_0 \div \Delta t_1$) starts at the sampling period, $\Delta t_0 = 0.05$ s. If the upper limit Δt_1 is chosen in the range $\Delta t_1 = 0.3 \div 2.5$ s in order to assure the lowest non-linearity error (represented here by the mean square error between the logarithm of the curve and the least-square line) and the highest intra-subject reliability, it was observed (and in the logarithmic plane it is well evident in Fig. 4) that a value of $\Delta t_1 = 0.3$ is always a good choice. As a consequence the short-term working region could be fixed a priori between 0.05 and 0.3 s.

2.4.1.2. Long-term working region. The l region ($\Delta t_2 \div \Delta t_3$) has been chosen of constant dimension (same number of points), and is optimally shifted from left to right to minimize the non-linearity error. The dimension was preliminarily estimated maximizing the repeatability of long-term parameters for each patient and experimental condition. As a consequence, 33 points were used for characterizing the l region in the whole data set.

Hence, the only design parameter that is not fixed a priori is the initial time lag of the long-term window, Δt_2. In Fig. 5 the non-linearity error is reported as a function of Δt_2, in the case of the representative trial presented in Figs. 1–3. The value corresponding to the minimum value of the curve in the range $\Delta t_2 = 0.3 \div 2.5$ s is chosen.

Fig. 4 shows that the present choice seems to be able to cope with the two main linear tracts present in the short-term and long-term regions of the stabilogram diffusion plot so improving repeatability. The same time-interval selection technique was used to estimate the parameters of both stochastic models. Of course, the interval selection is carried out either in the linear plane (SMP) or in the log–log plane (NSMP).

2.4.2. SMP estimation

The SMP, as defined in Eqs. (1) and (2), were computed by a piecewise linear parameterization of the linear and logarithmic stabilogram diffusion plots following the algorithm proposed by Collins and De Luca [16]. After time interval selection is carried out once in

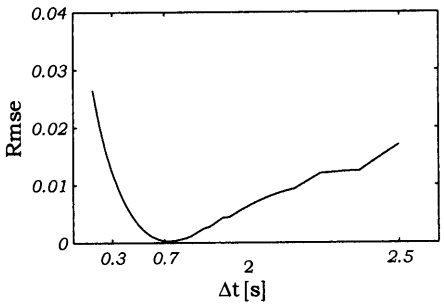

Fig. 5. Tuning of the parameter estimation technique. The only design parameter that is not fixed a priori is the lower limit of the long-term window, Δt_2. In figure is reported the root mean square of the residuals between the experimental curve and the best fitting line when Δt_2 is iterated in the range $0.3 \div 2.5$ s. The value corresponding to the minimum value of the curve is chosen.

the linear plane, four SMP are estimated from the linear stabilogram diffusion plots and two SMP, in the same intervals, from corresponding logarithmic stabilogram diffusion plots.

2.4.3. NSMP estimation

The overall best for the left and right side fittings (i.e. the minimum mean square error in the short- and long-term time windows) were independently found. A least-squares algorithm was used for the estimation of K_s, H_s, in the short-term region, and K_l, H_l in the long-term region. Initial time-lag for the log-term region was increased from 0.3 s step by step repeating each time the parameter and non-linearity error evaluation. The log–log diffusion plot for each individual trial was fitted with two least-squares best-fitting lines to capture the difference in the scaling exponent (and hence in the correlation between increments making up the experimental time series) of the initial and final region of the curve.

2.5. Statistical analysis

A total of 14 parameters were computed for each subject trial: four SSS, six SMP and four NSMP. Intra-individual repeatability of all these parameters was compared by an interexaminer reliability study. Intraclass correlation coefficients (ICC) were calculated to determine the degree of agreement between repeated measures of the parameters [23]. The random effects model was used, so that the proportion of variance of an observation due to subject-to-subject variability in error-free scores is expressed by the equation:

$$\mathrm{ICC} = \frac{N(\mathrm{SMS} - \mathrm{EMS})}{N\ \mathrm{SMS} + k\ \mathrm{RMS} + (Nk - N - k)\mathrm{EMS}} \qquad (7)$$

where N is the number of subjects, k is the number of repeated measures per subject, SMS, RMS and EMS are the between-subjects, between raters (trials) and error mean square, respectively.

The reliability of all the parameters was assessed following the general guidelines proposed by Fleiss [23] and also adopted by Collins and De Luca [12] in their early work:

ICC < 0.4 — poor reliability (P)

0.4 < ICC < 0.75 — fair to good reliability (F/G)

ICC > 0.75 — excellent reliability (E)

Analysis of variance (ANOVA) was performed on each parameter to highlight the differences between the visual conditions eo and ec.

Finally, Pearson correlation coefficients were computed for all parameters, and the degree of linear correlation was considered significant when $r \geq 0.90$ with both eyes open and eyes closed.

Table 2
Sensitivity to the visual conditions (mean values and standard deviations of the means for the three groups of parameters)[a]

		Vision	No vision	
SSS	MV (mm s^{-1})	9.87 ± 2.53	12.98 ± 4.01	**
	CEA (mm^2)	128.03 ± 61.30	178.08 ± 112.03	**
	FD	1.68 ± 0.06	1.74 ± 0.09	–[b]
	CF (Hz)	0.65 ± 0.10	0.67 ± 0.16	–
SMP	D_s (mm^2 s^{-1})	13.13 ± 7.10	23.33 ± 15.33	*
	D_l (mm^2 s^{-1})	2.44 ± 1.72	1.87 ± 1.68	–
	Δt_c (s)	1.28 ± 1.23	1.08 ± 0.44	–
	$\langle \Delta r^2 \rangle_c$ (mm^2)	28.02 ± 23.80	42.13 ± 24.03	**
	H_s	0.81 ± 0.03	0.81 ± 0.04	–
	H_l	0.10 ± 0.12	0.02 ± 0.08	*
NSMP	K_s (mm^2)	1.65 ± 0.28	1.88 ± 0.31	*
	K_l (mm^2)	1.25 ± 0.23	1.51 ± 0.28	*
	H_s	0.84 ± 0.02	0.84 ± 0.03	–
	H_l	0.21 ± 0.07	0.12 ± 0.06	*

[a] SSS, SMP as computed by Collins and De Luca [12], and NSMP. Values refer to different visual conditions and last column reports the level of significance of their difference computed with ANOVA.

[b] – no significance.

* $P < 0.001$.

** $P < 0.01$.

3. Results

The means and between-subjects standard deviations of all parameters within each visual condition are listed in Table 2. Last column reports the significance level computed by ANOVA of the hypothesis test that the two operating conditions, eyes open and eyes closed, have the same mean. Only comparisons with $P < 0.01$ were considered indicative of a statistically significant difference between the eye conditions.

The results obtained for summary statistic COP parameters are in accordance with those reported by Prieto et al. [7] for a population of healthy young adults: all SSS values increase when eyes are closed and sensitivities are similar, i.e. only MV and CEA reflect significant changes between the eo and ec conditions ($P < 0.01$).

As regards the SMP, Table 2 shows that the short-term diffusion coefficient, D_s, is larger than the long-term one, D_l, as predicted by Collins and De Luca [12] and this is true both in eo and ec conditions. But while the first increases with no vision ($P < 0.001$), the second tends to decrease, even if not significantly. It is worth noting that D_l was formerly used to pre-classify subjects into different groups and consequently explain visual integration in the postural control system according to different strategies [16]. The computation of the Romberg ratio $D_l(\mathrm{ec})/D_l(\mathrm{eo})$ did not prove the existence of two separate groups in our population and neither was it possible to identify a nearly bimodal distribution of the Romberg ratio, nor were the five repeated exper-

iments (the eo and ec consecutive trials) for the same subject uniquely classified. Hence, the explanation given in terms of a couple of possible integration strategies between postural inputs becomes a matter of doubt in the present population, based on this classification approach, because a same strategy would be expected in one subject over short periods of time.

The estimates of the critical point in time are somewhat different from the eo mean values obtained by Collins and De Luca [16] ($\Delta t_c \cong 0.9 \pm 0.2$ s) but are similar to the ones measured by Newell et al. [15] ($\Delta t_c = 1.38 \pm 1.36$ s) with three repeated trials on their student population. The mean value and the sign of the change of $\langle \Delta r^2 \rangle_c$ are consistent with the observations made by Collins and De Luca [16]. Finally, results similar to Collins and De Luca were obtained for the values of scaling exponents; compare the following values with the ones reported in Table 2: $H_s(\text{eo}) \cong H_s(\text{ec}) \cong 0.8 \pm 0.04$; $H_l(\text{eo}) \cong 0.3 \pm 0.08$; $H_l(\text{ec}) \cong 0.25 \pm 0.08$. Mean values of H_l are here slightly lower for both eo and ec conditions perhaps due to the presence of saturation in some trials and the longer duration of the trials. In fact, it is expected that after a sufficiently large time lag the stabilogram diffusion plots saturate to a constant value, because of the bounding given by feet support. Newell et al. [15] did not estimate the scaling exponents. In summary, it is remarkable that sensitivity to vision was found to be significant for the same group of parameters, that is D_s, $\langle \Delta r^2 \rangle_c$ and H_l, irrespective of the preclassification rule proposed by Collins and De Luca [16]. Different is the case of D_l because they found a moderate sensitivity ($P < 0.05$) only after the subdivision of subjects in two groups.

The bottom rows of Table 2 report the mean values and between-subjects standard deviations of NSMP. The only comparison that can be made with previous results concerns H_s and H_l. The different values with respect to SMP are due to the new parameterization technique that does not simply propagate the s and l best-fitting regions identified in the linear plane but optimize them directly on the logarithmic scale. The higher values of H_l reflect a more reliable estimate of the long-term correlation, which avoids the possible saturation from the working region. The increase in mean values of K_s and K_l denotes the general upward shift that is observed in stabilogram diffusion plots when eyes are closed.

The Pearson correlation coefficients were computed for all parameters with both eyes open and closed. All parameters belonging to a same group were uncorrelated except Δt_c and $\langle \Delta r^2 \rangle_c$ in SMP that were highly correlated with eo ($r = 0.94$, $P < 0.001$). The only result that was found to be significant between parameters of different groups concerned MV, K_s and D_s that were all correlated ($r > 0.95$, $P < 0.001$). For this reason, it appears that statistical mechanics parameters (both SMP and NSMP) added further information to the characterization of the posturographic signal with respect to summary statistic scores. The absence of correlation with CEA, FD and CF is indicative that their information either was discarded or was embedded in a non-linear fashion into new parameters.

The categorization of ICC into poor (P), fair to good (F/G) and excellent (E) leads to the results shown in Table 3 for the three groups of parameters. The NSMP are clearly more reliable than the SMP and the SSS. It is worth to note that the reliabilities obtained for the SMP are much worse than those reported by Collins and De Luca [12], that ranged between 0.62 for Δt_c and 0.9 for D_s. This is mainly due to the reduction of intra-subject variability that they obtained by averaging repeated stabilogram-diffusion plots. Furthermore, the proposed fitting procedure for the stabilogram diffusion plots was compared with the one that includes also the data points around the cut-off between the short-term and the long-term region (i.e. considers all points of the stabilogram diffusion function). The results obtained in terms of reliability of the estimates of H_s and H_l are worse than those presented in Table 3.

The ICCs of the NSMP are higher, and almost comparable with values obtained by averaged curves, because of the improved parameter extraction technique. Moreover, a limitation of SMP arises from the different reliability that was recorded with eo and ec (see Δt_c, $\langle \Delta r^2 \rangle_c$ and H_l) so that the use of a parameter should be carefully linked to specific operating conditions and this is not good for a robust parameterization. Critical time lag had a low ICC also when it was computed over ensemble trials [12].

Table 3
Reliability analysis (intraclass correlation coefficients and respective categorization for the repeated measurements of the parameters)[a]

		Vision		No vision	
SSS	MV	0.83	E	0.87	E
	CEA	0.58	F/G	0.70	F/G
	FD	0.53	F/G	0.71	F/G
	CF	0.56	F/G	0.80	E
SMP	D_s	0.79	E	0.79	E
	D_l	0.50	F/G	0.43	F/G
	Δt_c	0.23	P	0.63	F/G
	$\langle \Delta r^2 \rangle_c$	0.20	P	0.66	F/G
	H_s	0.61	F/G	0.65	F/G
	H_l	0.41	F/G	0.26	P
NSMP	K_s	0.85	E	0.88	E
	K_l	0.81	E	0.89	E
	H_s	0.83	E	0.88	E
	H_l	0.54	F/G	0.49	F/G

[a] SSS, SMP as computed by Collins and De Luca [12], and NSMP. Values refer to different visual conditions.

The four SSS that were chosen for this analysis were all sufficiently reliable, but it should be pointed out that when different SSS are selected to quantify sway, their reliability should be verified. In fact, some of the SSS proposed in literature are less reliable than the ones we considered in this study. It should be also pointed out that compared to SSS such as sway path and mean velocity, both SMP and NSMP are less sensitive to the sampling frequency because these SSS may be biased due to high frequency measurement and quantization noise [24]. A further factor that may influence the values and the reliabilities of the SSS, and only to a minor extent the SMP and NSMP, is the duration of the trial.

4. Discussion

Three major conclusions emerged from the present study. First, the stochastic model proposed by Collins and De Luca [12], although seminal for testing hypotheses on the nature of COP time series and clinically promising, may be further improved. A single theoretical framework can explain the data, and this has significant consequences on parameter reliability and experimental design. Second, stochastic parameters are more informative than summary statistic scores, even if they should be examined thoroughly and validated over time to assess their actual skill in capturing physiologically meaningful information. Third, an interpretation of stochastic analysis results in terms of motor control theory is intriguing but needs to be integrated with the view of the postural control system as a continuously regulated feedback system with a non-negligible mass in the controlled part [25,26].

4.1. Stochastic modeling

Newell et al. [15] pointed out a main problem arising from the application of the bounded, two-process random-walk model proposed by Collins and De Luca [12] for COP time series. The two different models proposed for the same data set make the approach not parsimonious and the variability in all the parameter estimates high, so that different stochastic approaches could be candidates to fit the data. For this reason, we went back to the definition of fractional Brownian motion proposed by Mandelbrot and Van Ness [17] and assessed the stochastic properties of the COP dynamics with the resultant four parameter non-linear model defined in Eq. (4). This avoided the approximation (and possible confusion) introduced by using the linear model of classical Brownian motion.

The more precise characterization of the fractional Brownian motion, together with a global reduction of complexity for the new model, and the definition of a new estimation technique optimized in the log–log plane allowed us to deal with more reliable estimates for all the single trials in the study. Increased reliability allows each parameter to be well captured even if fewer trials are taken. Collins and De Luca [12] faced this crucial aspect with the trial averaging technique and obtained (from three sets of ten trials) an improvement in the reliability of their parameters. We preferred instead to directly act on the quality of the single parameter and the effect was well evident (Table 3). The important consequence could be that of a facilitated experimental design and a strong reduction in the time spent for acquisitions. This reduces the occurrence of fatigue, mainly in subjects that, due to age or pathology, cannot afford long testing sessions.

Both reliability and sensitivity to visual conditions are larger for NSMP compared to SMP (Table 2). Also, the preclassification method used by Collins and De Luca [16] may be fragile. In fact, the classification of subjects into two groups was based only on the relative changes in the planar long-term effective diffusion coefficient but it is worth to note that such changes are related also to variations in the corresponding Hurst exponent, H_l. Hence, more care should be taken in the consequent physiological interpretation of the results.

4.2. Physiological meaning of parameters

Summary statistic COP parameters do not consider the dynamic characteristics of the COP motion over the base of support and for this reason they are less useful in the comprehension of the mechanisms that the central nervous system puts into play with the task of controlling posture. In contrast, statistical mechanics parameters (SMP and NSMP) can be related to the steady-state dynamic behavior of COP motion and quantify short- and long-term correlations that may be explained in terms of motor control theory [12].

The physiological meaning of the NSMP parameters is similar to SMP parameters. In particular, H explains the correlation between the step increments in that $H_s > 0.5$ denotes a short-term persistence, or tendency to persist in the same direction away in the COP motion, and $H_l < 0.5$ suggests an anti-persistence, i.e. a long-term tendency to return to initial position. Furthermore, K could be thought of as a generalized diffusion coefficient that equals $\log(2D)$ when $H = 0.5$, since $V_H = 1$. However, the known dependence of K on H allows us to compute values of D, through the analytical or numerical knowledge of V_H, that are quite different from previous estimations [10,12,14–16,19].

It is also worth noting that K_s (and D_s) were highly correlated with MV and each other. Since MV has been related to the stiffness of the system (i.e. the amount of regulatory activity associated with the level of stability achieved) [27], this confirms that the short-term offset

(and the short-term 'effective' diffusion coefficient) can be assumed as an indicator of the stochasticity level which is embedded in short lags. But while K (and D) changes over time-lags MV cannot account for any dynamics, and hence is not correlated with K_1 (and D_1), as well.

4.3. Motor control implications

Experimental stabilogram diffusion plots, when analyzed as fractional Brownian motions, disclose at least two kinds of dynamic behavior over different intervals of time. Collins and De Luca [19] explained such patterns in terms of open-loop and closed-loop control schemes, with feedback mechanisms, such as the visual, vestibular, and proprioceptive systems, acting only over long intervals of time. In fact, they associated the persistence behavior of COP motion in the short-term region ($H_s > 0.5$) with the action of an open-loop control system, and the long-term anti-persistence behavior ($H_s < 0.5$) with a closed-loop regulation. This hypothesis was emphasized in a successive paper where a continuous pinned polymer model of posture control was introduced [28]. Once more, the short-term open-loop paradigm was supported with the presence of delays or non-linearities in the feedback control system. However, another source of COP motion persistence over short intervals of time could be identified with the inertial properties of the human body or the gravity force action. But it should be remarked that, since both SMP and NSMP descend from a random-walk model of COP motion, they cannot account for the dynamics of the body as the controlled plant, and, consequently, none of them can directly prove any hypothesis on the control system nature. The step from stochastic process modeling of COP motion to physical (physiological) modeling can be filled up only by extrapolation. For example, Riley et al. [29] interpreted positive correlations over short time scales as the outcome of an 'exploratory' behavior, and negative correlations over long time scales as the outcome of a 'performatory' behavior of the system.

On the other side other authors captured the same two scaling regions with a closed-loop physical model in which the set-point is subject to a noisy dynamics [30] or with a feedback model with a finite time delay in a noisy environment [26]. For this reason, we think that the short-term process needs to be further investigated to address the effective role of gravity and inertia of the body. Their presence would suggest a control system that is always acting in a closed-loop, even if with different properties in the two regions. However this investigation was not on the focus of the present paper.

The present model left apart the explicit identification of a critical point in time that distinguishes the s and l regions. Newell et al. [15] questioned the functional significance of such a point and the way of estimating it through average ensembles adopted by Collins and De Luca. A 'dead zone' mechanism was suggested to justify the transition region over which this apparent decoupling takes place [19] but such issue was also differently addressed through continuous models [15,28] that overcome some instances of this separation. In this direction, it is remarkable that the present approach, through a piecewise identification of the two parameters of a novel non-linear model, may lead to simplify the experimental protocol and improve the clinical classification scheme. For this reason, it seems more realistic to turn future research in the direction of identifying a single continuous process for control of postural stability rather than two distinct components. A single mechanism model may allow a better fit of the stabilogram diffusion function, which will reduce model errors. A single mechanism will also allow describing with a unique framework the several, different synergies that a healthy subject activates for postural control.

Acknowledgements

The authors are grateful to Fay Horak, Roberto Piperno and Silvio Cavalcanti for the helpful discussions and suggestions. It is also a pleasure to thank Alessandro Tonini for the assistance during data acquisition and the thorough and constructive contribution of two anonymous reviewers. Work supported by Istituto Superiore di Sanità, Rome, Italy, first research project 'Function replacement, artificial organs and organ transplantation'.

References

[1] Dichgans J, Mauritz KH, Allum JHJ, Brandt T. Postural sway in normals and atactic patients: analysis of the stabilizing and destabilizing effects of vision. Agressologie 1976;17:15–24.
[2] Katoulis EC, Ebdon-Parry M, Hollis S, Harrison AJ, Vileikyte L, Kulkarni J, Boulton AJ. Postural instability in diabetic neuropathic patients at risk of foot ulceration. Diabet Med 1997;14:296–300.
[3] Baloh RW, Jacobson KJ, Beykirch K, Honrubia V. Static and dynamic posturography in patients with vestibular and cerebellar lesions. Arch Neurol 1998;55:649–54.
[4] O'Connell M, George K, Stock D. Postural sway and balance testing: a comparison of normal and anterior cruciate ligament deficient knees. Gait Posture 1998;8:136–42.
[5] Berg KO, Maki BE, Williams JI, Holliday PJ, Wood-Dauphinee SL. Clinical and laboratory measures of postural balance in an elderly population. Arch Phys Med Rehabil 1992;73:1073–80.
[6] Prieto TE, Myklebust JB, Myklebust BM. Characterization and modeling of postural steadiness in the elderly: a review. IEEE Trans Rehab Eng 1993;1:26–34.
[7] Prieto TE, Myklebust JB, Hoffmann RG, Lovett EG, Myklebust BM. Measures of postural steadiness: differences between healthy young and elderly adults. IEEE Trans Biomed Eng 1996;43:956–66.

[8] Maki BE, Holliday PJ, Topper AK. A prospective study of postural balance and risk of falling in an ambulatory and independent elderly population. J Gerontol 1994;49:72–84.
[9] Kapteyn TS, Bles W, Njiokiktjien CJ, Kodde L, Massen CH, Mol JM. Standardization in platform stabilometry being a part of posturography. Agressologie 1983;24:321–6.
[10] Collins JJ, De Luca CJ, Burrows A, Lipsitz LA. Age-related changes in open-loop and closed-loop postural control mechanisms. Exp Brain Res 1995;104:480–92.
[11] Yamada N. Chaotic swaying of the upright posture. Hum Mov Sci 1995;14:711–26.
[12] Collins JJ, De Luca CJ. Open-loop and closed-loop control of posture: a random-walk analysis of center-of-pressure trajectories. Exp Brain Res 1993;95:308–18.
[13] Harris CM, Wolpert DM. Signal-dependent noise determines motor planning. Nature 1998;394:780–4.
[14] Mitchell SL, Collins JJ, De Luca CJ, Burrows A, Lipsitz LA. Open-loop and closed-loop postural control mechanisms in Parkinson's disease: increased mediolateral activity during quiet standing. Neurosci Lett 1995;197:133–6.
[15] Newell KM, Slobounov SM, Slobounova ES, Molenaar PC. Stochastic processes in postural center-of-pressure profiles. Exp Brain Res 1997;113:158–64.
[16] Collins JJ, De Luca CJ. The effects of visual input on open-loop and closed-loop postural control mechanisms. Exp Brain Res 1995;103:151–63.
[17] Mandelbrot BB, Van Ness JW. Fractional Brownian motions, fractional noises and applications. SIAM Rev 1968;10:422–37.
[18] Katz MJ, George EB. Fractals and the analysis of growth path. Bull Math Biol 1985;47:273–86.
[19] Collins JJ, De Luca CJ. Upright, correlated random-walks — a statistical-biomechanics approach to the human postural control-system. Chaos 1995;5:57–63.
[20] Kaplan LM, Kuo CCJ. Extending self-similarity for fractional Brownian motion. IEEE Trans Sign Proc 1994;42:3526–30.
[21] Carroll JP, Freedman W. Nonstationary properties of postural sway. J Biomech 1993;26:409–16.
[22] Schumann T, Redfern MS, Furman JM, el-Jaroudi A, Chaparro LF. Time-frequency analysis of postural sway. J Biomech 1995;28:603–7.
[23] Fleiss JL. The Design and Analysis of Clinical Experiments. New York: Wiley, 1986.
[24] Granat MH, Kirkwood CA, Andrews BJ. Problem with the use of total distance travelled and average speed as measures of postural sway. Med Biol Eng Comput 1990;28:601–2.
[25] Johansson R, Magnusson M, Akesson M. Identification of human postural dynamics. IEEE Trans Biomed Eng 1988;35:858–69.
[26] Peterka RJ. Stabilogram diffusion analysis results are predicted by a simple postural control model. In: Keshner EA, editor. Identifying Control Mechanisms for Postural Behaviors. Los Angeles, CA: Society for Neuroscience Satellite Meeting, 1998:73–4.
[27] Maki BE, Holliday PJ, Fernie GR. Aging and postural control. A comparison of spontaneous- and induced-sway balance tests. J Am Geriatr Soc 1990;38:1–9.
[28] Chow CC, Collins CJ. Pinned polymer model of posture control. Phys Rev E 1995;52:907–12.
[29] Riley MA, Mitra S, Stoffregen TA, Turvey MT. Influences of body lean and vision on unperturbed postural sway. Mot Control 1997;1:229–46.
[30] Dijkstra TMH. Dynamics of frame of reference captures the two scaling regimes of human postural control. Soc Neurosci Abstr 1998;24(2):1768.